



PCCP

**Significance of the Surface Silica/Alumina Ratio and Surface Termination on the Immersion Freezing of ZSM-5 Zeolites**

Journal:	<i>Physical Chemistry Chemical Physics</i>
Manuscript ID	CP-ART-11-2022-005466.R1
Article Type:	Paper
Date Submitted by the Author:	23-Mar-2023
Complete List of Authors:	Marak, Katherine E.; Penn State University, Chemistry Nandy, Lucy; Penn State University, Chemistry Jain, Divya; Penn State University, Chemistry Freedman, Miriam; The Pennsylvania State University, Chemistry

SCHOLARONE™  
Manuscripts

**Significance of the Surface Silica/Alumina Ratio and Surface Termination on the  
Immersion Freezing of ZSM-5 Zeolites**

Katherine E. Marak<sup>1,#</sup>, Lucy Nandy<sup>1,#</sup>, Divya Jain<sup>1,&</sup>, Miriam Arak Freedman<sup>1,2\*</sup>

*1) Department of Chemistry and 2) Department of Meteorology and Atmospheric Science*

*The Pennsylvania State University, University Park, PA 16802, USA*

Manuscript submitted to *Physical Chemistry Chemical Physics*

\* To whom all correspondence should be addressed: [maf43@psu.edu](mailto:maf43@psu.edu)

# These authors have contributed equally to this work.

& Present address: Ernst & Young, LLP, Houston, TX 77010

Abstract:

Heterogeneous ice nucleation in the atmosphere impacts climate, but the magnitude of the effect of ice clouds on radiative forcing is uncertain. Surfaces that promote ice nucleation are varied. Because O, Si, and Al are the most abundant elements in the Earth's crust, understanding how the Si:Al ratio impacts the ice nucleation activity of aluminosilicates through exploration of synthetic ZSM-5 samples provides a good model system. This paper investigates the immersion freezing of ZSM-5 samples with varying Si:Al ratios. Ice nucleation temperature increases with increasing surface Al content. Additionally, when ammonium, a common cation in aerosol particles, is adsorbed to the zeolite surface, initial freezing temperatures are reduced by up to 6 °C in comparison to proton-terminated zeolite surfaces. This large decrease in ice nucleation activity in the presence of ammonium suggests that the cation can interact with the surface to block or

modify active sites. Our results on synthetic samples in which the surface composition is tunable gives insight into the role of surfaces in heterogeneous ice nucleation processes in the atmosphere. We emphasize the importance of examining surface chemical heterogeneities in ice nucleating particles that could result from a variety of aging pathways for a deeper understanding of the freezing mechanism.

### **Introduction:**

Heterogeneous ice nucleation is significant for the formation of ice cloud particles in the troposphere and stratosphere.<sup>1,2</sup> Ice clouds in the atmosphere have a significantly different impact on radiative forcing than liquid water clouds, with ice clouds having a slight net warming effect, and water clouds having a cooling effect, although the magnitude of these effects can vary depending on the data collection method.<sup>3</sup> Aerosol particles that comprise the surfaces for heterogeneous nucleation are incredibly diverse, and this leads to a large range of ice nucleation temperatures above the homogeneous freezing limit of  $-38\text{ }^{\circ}\text{C}$  and as warm as  $-2.5\text{ }^{\circ}\text{C}$ .<sup>4,5</sup> The surface features that dictate the heterogeneous freezing process are currently being explored and include: crystallinity, crystal structure, oxidation, surface functionality, roughness, coatings and porosity.<sup>6</sup> Pruppacher and Klett in 1978 had first suggested that in addition to particle size and water-insolubility requirements for ice nucleation, functional groups, crystal structure, active sites like morphological inhomogeneity (surface crack, step or cavity), chemical inhomogeneity (hydrophilic ion) and electrical inhomogeneity (other than ions) also play a role in ice nucleation.<sup>6</sup> We have specifically been studying the crystallinity and crystal structure,<sup>7</sup> oxidation, surface functionality,<sup>8</sup> roughness, coatings and porosity effects<sup>9</sup> on ice nucleation. The relative

significance of these features is critical to understanding the diversity of ice nuclei in the atmosphere.

There are several heterogeneous freezing pathways for ice, including contact freezing, condensation freezing, pore condensation freezing, and immersion freezing,<sup>10–12</sup> the latter of which will be studied in this work. Immersion freezing is a mechanism of ice nucleation which involves a solid particle suspended in a supercooled liquid water droplet. The surface of this particle lowers the activation barrier to allow ice to form at warmer temperatures than homogeneous water droplets.

Aluminosilicates are highly abundant mineral types in the atmosphere, and consist of feldspars (e.g. K-feldspar, albite and anorthite) and clay minerals (e.g. kaolinite, illite, dolomite, and montmorillonite) which are found in mineral dust samples around the globe.<sup>13</sup> Alkali feldspars have been extensively studied for their ice nucleation activity.<sup>14–23</sup> The ice nucleation activity varies between feldspar samples, with K-rich samples having a consistent high activity; Na-rich samples nucleating ice at high activity, but losing that activity over time in water; and calcium rich samples having the lowest activity.<sup>23</sup> It has also been shown that some aluminosilicates are not stable in water. Prolonged immersion in water can cause the depletion of Al content, favoring Si-rich amorphous surfaces, which consequently reduces the ice nucleation temperatures.<sup>22</sup> Clay aluminosilicate minerals have also been extensively studied both theoretically<sup>24–28</sup> and experimentally.<sup>29–35</sup> Kaolinite is a common clay mineral and has a unique arrangement of a layer of alumina tetrahedra with hydroxyl groups and a layer of silica tetrahedra with bound oxygen groups.<sup>36</sup> The alumina basal plane is more ice active than the silica basal plane, and in fact, Soni and Patey showed in computational studies that removing the Si layer does not change the ice nucleation activity of the kaolinite by the alumina layer.<sup>37,38</sup> Alumina can have a variety of different

activities depending on the structure of the alumina and its crystallinity.<sup>7</sup> Even though gibbsite is structurally close to the hydrophilic<sup>39</sup> alumina basal plane of kaolinite, both from simulations and experiments, it has been found to be a relatively poor ice nucleating particle.<sup>7,37,40</sup> However, the alumina basal plane of kaolinite has been found to be polar,<sup>41</sup> amphoteric,<sup>38</sup> and therefore, an effective ice nucleating particle,<sup>27,42</sup> but the effectiveness may not be because of its good epitaxial match with the basal face of ice.<sup>39</sup> The ice nucleating effectiveness of kaolinite is consistent with experimental studies<sup>40</sup> although ice nucleation on basal or edge planes have not been distinguished extensively in laboratory settings. Wang et al. demonstrated that the edge surfaces are preferential ice nucleation sites over the basal plane using electron microscopy,<sup>43</sup> and Freedman suggested possibility of ice nucleation on the edge surface defects as well.<sup>28</sup> Studies performed with aluminosilicate minerals suggests that in addition to cation effects, the placement and quantity of silica and alumina can play a role in the ice nucleation activity.<sup>26,44,45</sup>

Zeolites are unique forms of porous silicates, with additional metals possible for the framework, commonly aluminum. Aluminosilicate zeolites have a natural negative charge from the  $[\text{SiO}_4]^{-4}$  and  $[\text{AlO}_4]^{-5}$  tetrahedra which combine by sharing corner(s) to make different structures in a porous framework with a structural formula of  $\text{M}_{x/n}[(\text{AlO}_2)_x(\text{SiO}_2)_y] \cdot w\text{H}_2\text{O}$ .<sup>46,47</sup> In this formula, M is a cation with valence (n), w is the amount of water incorporated in the lattice and x and y are the number of tetrahedra present. The negative charge is balanced by a cation that is strongly adsorbed in the small honeycomb-like pore network. Natural zeolites will have alkali metal cations, while synthetic zeolites can have a wide range of cations, including  $\text{H}^+$  and  $\text{NH}_4^+$ . The Commission for Natural Zeolites has identified the structure of 65 naturally occurring zeolites as of May 2022.<sup>48</sup> Natural zeolites have been used in purification processes in water and gas.<sup>49–52</sup> However, synthetic zeolites are more common in industrial and synthetic uses because there is

more control over properties like pore size, cation composition, and Si:Al ratio. 246 synthetic zeolite structures are recognized by the International Zeolite Association as of July 2022, but scholars working on novel zeolite forms have suggested that as many as 4 million unique structures are possible.<sup>53,54</sup> The pores of zeolites have also been used to study ice nucleation in confined spaces, with distinct homogeneous freezing in mesoporous cavities and heterogeneous freezing in surface mesopores.<sup>55</sup>

ZSM-5 is a class of synthetic zeolite whose structure was first identified in 1978.<sup>46</sup> It is described as isostructural to silicalite, with two types of intersecting channels with 10-membered ring openings of around 0.55 nm (Figure 1a).<sup>56</sup> The porous channels formed in the zeolite can clearly be seen in Figure 1b and Figure 1c which show a transparent surface framework wrap over the zeolite on the both the ac and bc planes. In ZSM-5 samples with a mix of silica and alumina tetrahedra, alumina concentration is enhanced near the surface of the zeolite.<sup>57</sup> The ratio of silica to alumina in ZSM-5 has been shown to affect the acidity and hydration of the zeolite, with acid sites and adsorbed water decreasing with increasing Si:Al ratios.<sup>58</sup>

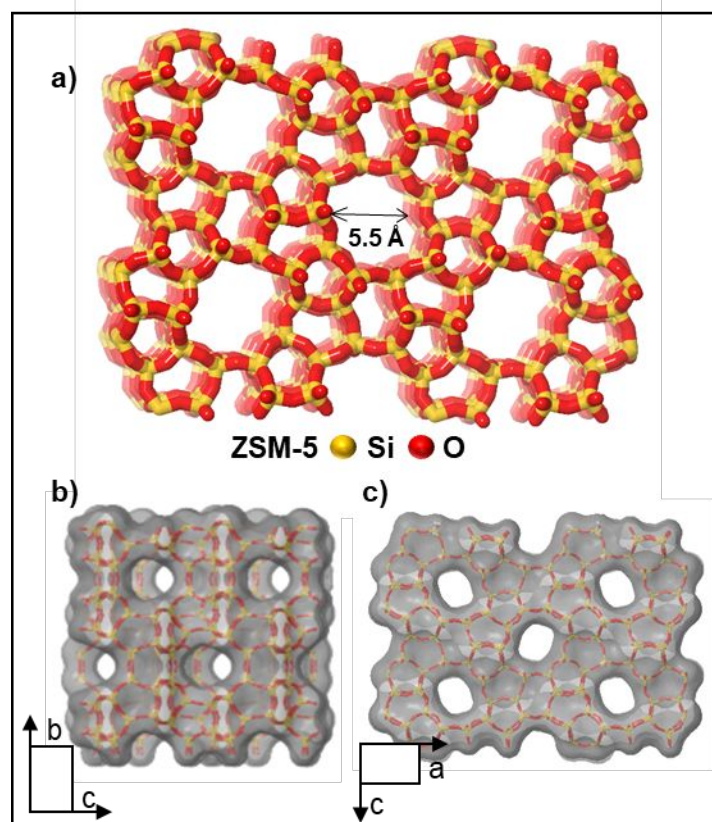


Figure 1: a) Lattice Structure of ZSM-5 type zeolite with oxygen and silicon atoms represented. The channel pore size is labeled. b) Transparent surface framework wrap over the bc plane of the ZSM-5 lattice c) Transparent surface framework wrap over the ac plane of the ZSM-5 lattice. The figures were made with data and the program JSmol from the International Zeolite Association.<sup>54</sup>

The large variety of Si:Al ratios for ZSM-5 samples make this type of zeolite an ideal system to study the role that composition plays on the ice nucleation activity of aluminosilicates. Additionally, ammonium is a common cation of ZSM-5 particles as well as a common atmospheric aerosol component. We have investigated the ice nucleation activity of four ZSM-5 samples ranging from all silicate to a 20:1 ratio of Si:Al, as well as three samples terminated with ammonium cations ( $\text{NH}_4$ -ZSM-5) rather than proton surface adsorbates. Our goal is to see how

increasing amounts of aluminum affect the ice nucleation activity, and if that activity is affected by the presence of ammonium on the surface.

### **Experimental:**

#### Materials:

The samples ZSM-5-20 (MR-25), ZSM-5-28 (P-117), ZSM-5-513 (P-360) and ZSM-5-Si (P-38) were purchased from ACS Materials (the product codes are in parentheses). The ammonium ZSM-5 samples were purchased from Thermo Scientific, ZSM-5-26 (CAS No. 1318-02-1), and Zeolyst ZSM-5-26 (CBV 5524G) and ZSM-5-33 (CBV 8014). All ZSM-5 samples have a porous structure with a ring opening of 0.55 nm. The ZSM-5 samples were purchased with different ratios of silica to alumina. However, the ZSM-5 samples in this paper will be referred to by their Si:Al ratio on the surface as determined by XPS rather than the manufacturer's value for the bulk Si:Al ratio (Table 1). Samples were used without further modification.

#### Material Characterization:

The surface areas of the samples were determined using Brunauer–Emmett–Teller (BET)-ASAP 2020 Automated Surface Area and Porosimetry System and nitrogen gas. The composition of these samples was verified using X-ray photoelectron spectroscopy (XPS). XPS experiments were performed using a Physical Electronics VersaProbe II instrument equipped with a monochromatic Al K $\alpha$  x-ray source ( $h\nu = 1,486.6$  eV) and a concentric hemispherical analyzer. The XPS experiments were performed on the sample surface plane at a typical sampling depth of 3-6 nm (95% of the signal originated from this depth or shallower). Since this is a surface technique, the composition may vary from the bulk. The samples were confirmed to be crystalline



using a Malvern Panalytical Empyrean X-Ray Diffractometer (XRD) with a powder sample stage and a background silica sample holder.

Ice nucleation chamber:

The immersion chamber used was first described by Alstadt et al.<sup>9</sup> The chamber consists of a copper block inside of an aluminum housing with a glass top for viewing. The copper block holds a hydrophobic coverslip containing the sample. For each sample, at least 100 droplets of 2 $\mu$ L from at least two solutions of 0.02 w/v% are analyzed. The samples are suspended in UHPLC water (Thermo Scientific) and pipetted onto a hydrophobic glass slide using a micropipette. The copper block is cooled using a stream of nitrogen gas that has been cooled by liquid nitrogen. The ice nucleation chamber is under a nitrogen atmosphere with a gentle stream of N<sub>2</sub> purging the chamber. The rate is controlled by a flowmeter and for these experiments was set to -3°C/min. This rate was chosen to ensure that the trial would complete before detectable droplet evaporation. Temperature is read using a K-type thermocouple and an PID controller (Omega). Images are taken using a camera set above the chamber for every half degree cooled and the sample is illuminated from above. Between trials, the chamber returns to room temperature.

Data analysis:

The analysis of our data generally follows the method of O'Sullivan et al. adapted from work by Vali et al.<sup>59,60</sup> Frozen fraction,  $F(T)$  for each trial is determined at each temperature using the following equation

$$F(T) = \frac{n(T)}{N} \quad (1)$$

where  $n(T)$  is the number of droplets frozen at a given temperature and  $N$  is the total number of droplets in the trial.

The  $F(T)$  is then converted to  $K(T)$  according to

$$K(T) = \frac{-\ln(1 - F(T))}{V} \quad (2)$$

which is the number of active sites in a mL of solution,  $V$ , at a given temperature. During this step, the error between trials of the same material is calculated using the standard deviation. The  $K(T)$  of water is also calculated and is subtracted from the  $K(T)$  values of our samples.

The surface area of our samples is significant due to their porous nature. The value  $n_s$ , the active sites per  $\text{cm}^2$  of the sample surface, is calculated from the net  $K(T)$  for each sample using the following equation

$$n_s = K(T) \times C^{-1} \quad (3)$$

where  $C$  is the total surface area in a given volume, and is calculated using the BET surface and the mass percent of zeolites in each experiment.

### Results and Discussion:

ZSM-5 samples were purchased with a range of reported Si:Al ratios as shown in Table 1 under the “Si:Al bulk” column, but the immersion freezing data in Figure 2 did not correlate to these values. Rather, we found that the Si:Al ratio found at the surface of the ZSM-5 samples using XPS was markedly different from the Si:Al ratios reported in bulk, with a range of 20 to 513. One sample, ZSM-5-Si, was even expected to have an Si:Al ratio of 38 but instead showed no aluminum in XPS and thus only contains silica at the surface.

Table 1: ZSM-5 Sample Composition

Sample <sup>a</sup>	XPS Al	XPS Si	Si:Al Bulk <sup>b</sup>	Si:Al XPS <sup>c</sup>	Cation
ZSM-5-20	1.4	29.2	25	20	H
ZSM-5-Si	-	31	38	-	H
ZSM-5-28	1.1	30.1	117	28	H
ZSM-5-513	0.1	28.5	360	513	H
ZSM-5-26	1.1	28.7	2	26	NH <sub>4</sub>
ZSM-5-24	1.2	29.1	50	24	NH <sub>4</sub>
ZSM-5-33	0.9	29.4	80	33	NH <sub>4</sub>

<sup>a</sup>Note that we have assigned names for the samples based on the XPS data. Discrepancies between the Si:Al XPS column and the XPS Al and Si columns are a result of the significant figures retained. <sup>b</sup>value reported by the manufacturer. <sup>c</sup>Si:Al XPS is the ratio of the XPS Al column to the XPS Si column

The immersion freezing data shown in figure 2a demonstrates a clear pattern of increasing ice nucleation activity with increasing surface aluminum content. Samples ZSM-5-20 and ZSM-5-28 begin freezing at -9 and -9.5 °C respectively and had fifty percent of the droplets frozen by -12.5 and -13 °C respectively. ZSM-5-513 which has significantly higher percentage of silica began freezing at -13 °C and was fifty percent frozen at -19°C. ZSM-5-Si, presumably all silica at the surface, did not begin freezing until -15°C and was fifty percent frozen at -24.5°C. The  $n_s$  data, Figure 2b, also shows that there are more ice active sites on samples with higher alumina content at all temperatures. The error shown in Figure 2b represents the standard deviation between trials, with upper and lower error being the same value, however the lower error bars will seem larger and cannot always be expressed due to the log scale.

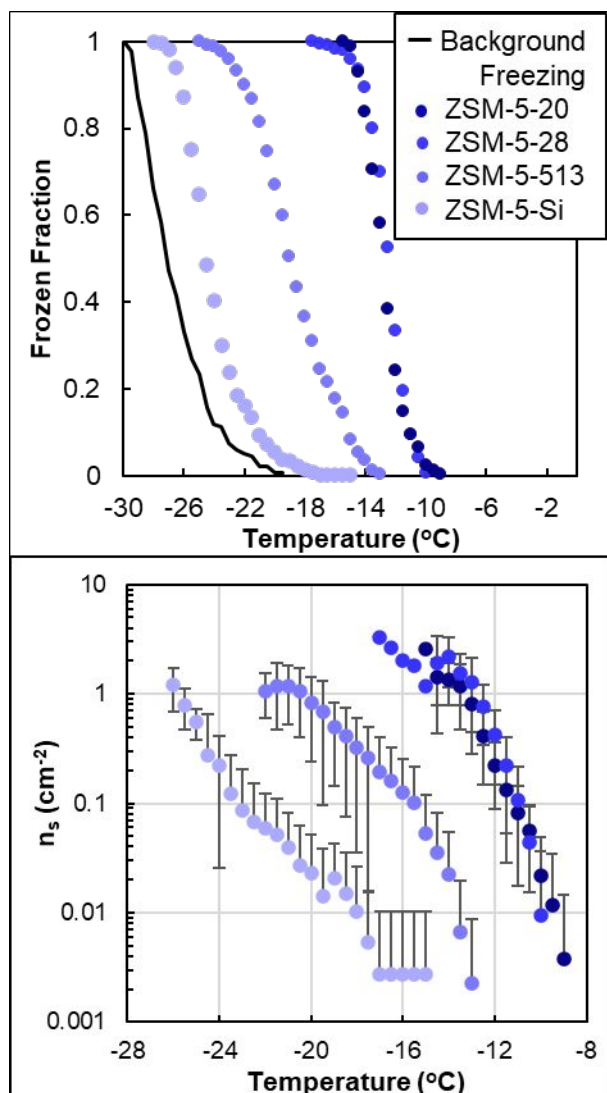


Figure 2. a) Frozen Fraction of ZSM-5 series as a function of temperature. b) Ice active site density,  $n_s$  of ZSM-5 series, as a function of temperature. The contribution from the ice nucleation of background water is removed and error is shown as the standard deviation between trials. The same legend is used for both graphs.

The freezing temperatures,  $T_{10}$ ,  $T_{50}$ , and  $T_{90}$ , representing the temperature that a given percentage, 10, 50, and 90%, of droplets has frozen is plotted for each zeolite in Figure 3. Viewing the data in this way helps to simplify the data to better compare values. Specifically,  $T_{10}$  is a more

reliable metric for characterizing a samples' initial freezing, as a single droplet freezing in a trial can suggest a high initial freezing temperature, while the bulk varies from this temperature. For example, in Figure 2a the initial freezing temperature of ZSM-5-Si is  $-15\text{ }^{\circ}\text{C}$  while the  $T_{10}$  is  $-21.5\text{ }^{\circ}\text{C}$ . This staggering  $6.5\text{ }^{\circ}\text{C}$  difference is likely due to a few droplets and does not accurately portray the freezing of the material. Additionally, looking at the temperatures for  $T_{10}$ ,  $T_{50}$  and  $T_{90}$  allows for an estimation of the slope of the curve due to freezing droplets. This slope can be used to interpret the uniformity of the active sites in a sample, with shallower slopes being more uniform. In the case of these zeolite samples, the slopes are similar, with ZSM-5-513 having the least uniformity of active sites.

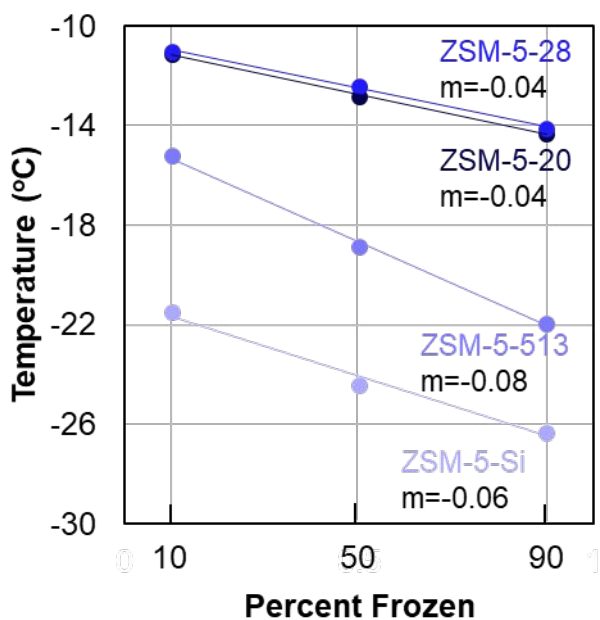


Figure 3. The temperature values  $T_{10}$ ,  $T_{50}$ , and  $T_{90}$  of ZSM-5-20, ZSM-5-28, ZSM-513 and ZSM-5-Si with the slopes calculated as explained in the text.

The significance of the Si:Al ratio on ice nucleation activity is not necessarily surprising considering the ice nucleation activity of pure porous silica and alumina samples. Porous alumina

can have active sites at temperatures as warm as  $-5\text{ }^{\circ}\text{C}$  for immersion freezing, while most porous silica is very poor at nucleating ice in immersion freezing with initial freezing temperatures of  $-15$  to  $-18\text{ }^{\circ}\text{C}$ .<sup>8,61</sup> Since zeolites are a combination of silica and alumina, we hypothesize that the active sites at warmer temperatures are coming from the more active alumina component rather than the less active silica. Similarly, the Al faces of the clay aluminosilicate mineral kaolinite are more ice active than the Si faces.<sup>38</sup> Additionally, it has been shown for ZSM-5 samples that total acid sites and water adsorption decrease with increasing Si/Al ratio and these acid sites are directly attributed to the tetrahedral Al.<sup>58,62</sup> The decrease in ice nucleation activity with decreasing Si/Al ratio at the surface may also suggest that Brønsted acid sites on tetrahedral aluminum surfaces interact with water near the surface in a way that is preferential for ice nucleation. Our findings add to the body of modeling studies that suggest the alumina content of aluminosilicate minerals is more important than the silica content for ice nucleation activity. This finding could be because of either the polar and amphoteric nature of the alumina basal plane<sup>38,41</sup> or defects on the edge<sup>43</sup> or both. A good epitaxial lattice match may not be the only reason for alumina basal plane to be more active.<sup>39</sup> For example, gibbsite that has no silica has been found to be a relatively poor ice nucleating particle even though it is geometrically identical to the alumina basal plane of kaolinite, which is an efficient ice nucleating particle.<sup>63</sup> On the other hand, quartz that has no alumina has been found to be a good ice nucleating particle. The reason may not be due to a lattice-matching mechanism as it shows a diverse ice-nucleation behavior.<sup>64–66</sup> Quartz could have a variety of ice active site densities and properties, that may deactivate due to aging.<sup>22</sup> Natural quartz samples and milled quartz samples could have defects in the crystal structure that may lead to more ice active sites, and therefore, experimental studies report quartz as a good ice nucleating particle.<sup>19,67</sup> Similarly, feldspars (aluminosilicates with tetrahedrally coordinated aluminum and silicon) have a range of

ice nucleating activity in the order microcline > albite > plagioclase.<sup>23,40</sup> Aluminosilicate clay minerals (aluminosilicates that have layered structures) also demonstrate a diverse ice-nucleation behavior in the order illite > montmorillonite > kaolinite.<sup>19,32,68</sup> The bulk Si/Al ratio for the mentioned aluminosilicates (feldspars and clay minerals) vary from 1 to 3, although the ratio on the surface of these samples has not been measured/reported. Hence, a direct correlation of the surface elemental composition with the ice nucleation efficiency cannot be derived. In addition, most of these samples have diverse surface properties, and may not be directly comparable to synthetic zeolites studied in this paper where we have isolated one property.

In the process of making ZSM-5, a cation must be present to balance the native negative charge of the aluminosilicate lattice. These cations are generally alkali metal ions, protons, or ammonium ions. The ice nucleation activity of three samples of NH<sub>4</sub>-ZSM-5 with similar Si:Al ratios (24-33) were characterized. The results shown in Figure 4a display a significant decrease in freezing temperatures for the ammonium samples compared to the ones with protons as the cation with similar Si:Al ratios (20,28). The initial freezing temperature varies by almost 6 °C and the fifty percent frozen by more than 8 °C on average between the ammonium ZSM-5 samples and the H<sup>+</sup> ones. This considerable difference suggests that the ammonium ion is interacting with the surface of the zeolite and potentially blocking or changing active sites which will be discussed below.

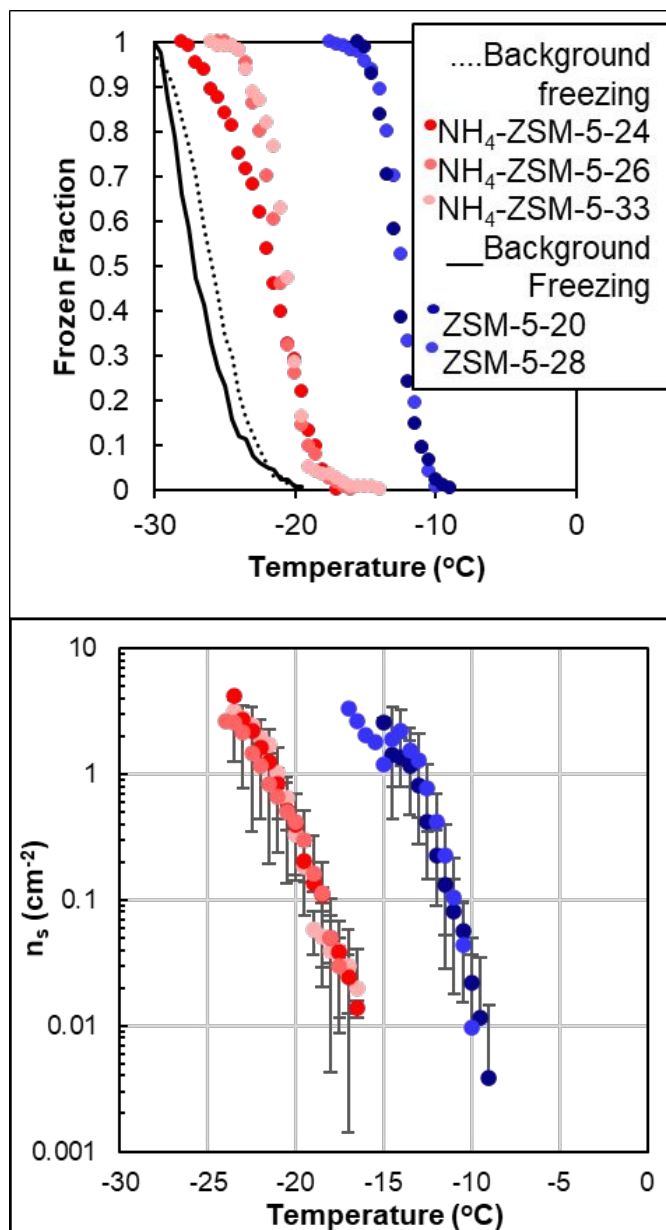


Figure 4: a) Frozen fraction of ZSM-5 samples with Si:Al between 20-32 with ammonium cations (red) and with protons (blue) as a function of temperature. b) Ice active site density,  $n_s$  of ZSM-5 series, as a function of temperature. The contribution from the ice nucleation of background water is removed and error is shown as the standard deviation between trials. The same legend is used for both graphs.



After calculating active sites and normalizing for the surface area ( $n_s$ ) in Figure 4b, the large decrease in activity with strongly bound ammonium cations is clear from the decrease in active sites. Also, in Figure 4b we can see that the H-ZSM-5 samples have completed freezing at  $-17^\circ\text{C}$  while the  $\text{NH}_4$ -ZSM-5 samples do not begin freezing until  $-16.5^\circ\text{C}$ . This disparity means that there are no active sites in the  $\text{NH}_4$ -ZSM-5 samples during nearly the entire temperature range that the H-ZSM-5 samples froze in. Additionally, the  $T_{10}$ ,  $T_{50}$ , and  $T_{90}$  of the  $\text{NH}_4$ -ZSM-5 zeolite samples are plotted in Figure 5 with the slopes. The slopes are very similar to the values of the H-ZSM-5 samples shown in Figure 3, suggesting that they have a similar uniformity of active sites. The lowest slope of all of the samples is for  $\text{NH}_4$ -ZSM-5-26 with a slope of  $-0.09^\circ\text{C}$  per fraction frozen which would make it the least uniform for active sites.

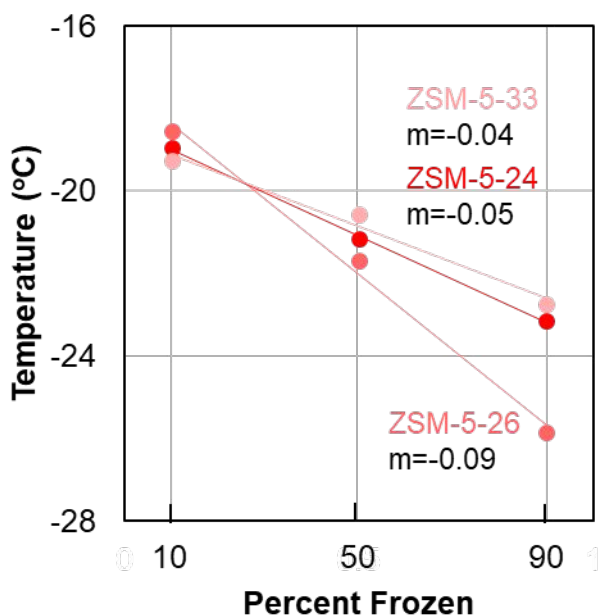


Figure 5: Temperature values,  $T_{10}$ ,  $T_{50}$ , and  $T_{90}$ , of  $\text{NH}_4$ -ZSM-5 samples with slopes at 10, 50, and 90 percent frozen.

The decrease in ice nucleation activity with the presence of ammonium may be due to the differences in hydrogen bonding interactions between water and protons vs. water and ammonium or that ammonium is a larger cation and preferentially interacts with Al which may block active sites. The freezing effects of ammonium have been studied for several materials, and generally ammonium reduces freezing according to the change in water activity like most ionic species.<sup>69</sup> However, Whale et al. has demonstrated the anomalous effect that ammonium can have on ice nucleation activity for some materials, arguing that in some cases ammonium can enhance the ice nucleation activity by reducing the charge on the surface and correcting strong ordering of water by the surface that is unfavorable for ice formation.<sup>70</sup> However, our ZSM-5 samples do not show this anomalous behavior with ammonium, and instead behave like most materials investigated by Whale et al., showing negative effects to ice nucleation activity from ammonium on the surface of the particle.<sup>69,70</sup> Water interactions with the surface are what drives heterogeneous ice nucleation, and ammonium has more hydrogen bonding opportunities compared to a proton, so we expect it to interact strongly with water. However, in some cases, a surface strongly adsorbing water negatively impacts the ice nucleation activity, because the water is held in unfavorable pre-ice structures.<sup>70,71</sup> Another possible explanation is that the ammonium is blocking active sites on the zeolite surface by interacting with the alumina. The adsorption of ammonium blocks aluminum surface sites of ZSM-5 by hydrogen bonding with alumina sites preferentially over silica sites.<sup>72</sup> Blocking the alumina active sites with adsorbed ammonium would reduce the freezing activity which is related to the ratio of Si:Al at the surface. By reducing available Al at the surface with ammonia blocking alumina sites, the Si:Al ratio would increase, and the freezing activity would decrease. We have discussed further on the anomalous behavior of ammonium as well as the influence of ion-specific effect on aluminosilicates as follows.

Depending on the type of the ice nucleating particle, the surface heterogeneities may change providing a better or a worse surface for interaction with liquid water, and therefore, ice nucleation. Dilute ammonium salt concentrations led to an increase in the ice nucleation efficiency in feldspars, kaolinite and montmorillonite<sup>40,69,73</sup> either by ion exchange or by adsorption of the ammonium cation onto the surface. Enhancement of heterogeneous ice nucleation on aluminosilicates is exceptional in the fact that it deviates from colligative effects of salts. In contrast, Arizona Test Dust samples showed a suppressed ice nucleation at warmer temperatures and no effect at cooler temperatures by ammonium sulfate.<sup>69</sup> In addition, Asian dust and aged Asian dust samples were studied to find no statistically significant difference in ice nucleation active site densities between the samples.<sup>74</sup> For the synthetic zeolite samples in this study, the surface elemental Si/Al ratios are much higher than the natural aluminosilicates generally studied. The differences in  $H^+$ ,  $NH_4^+$  and/or other cations, if any, normalized by the Al might be affecting the ice nucleating activity. Further studies are required to provide more insights. Moreover, the concentration of  $NH_4^+$  is an important factor in dictating the ice nucleation enhancement.<sup>70</sup> In a computational study, even in a dilute ammonium salt solution, ice nucleation enhancement was not observed in kaolinite.<sup>25</sup> Molecular dynamics simulations have also been done on microcline only to find no change in ice nucleation on  $NH_4^+$  adsorbed/exchanged microcline surfaces.<sup>75</sup> All these findings call for further studies on a microscopic level to understand the ice nucleation mechanism on aluminosilicate surfaces.

Beyond ammonium, surface cation exchange or adsorption has been shown to have an influence on heterogeneous ice nucleation in aluminosilicates. Generally, anions tend to have a greater effect on the orientation of water than cations.<sup>76,77</sup> However, different cations may also organize water differently by the Hofmeister effect.<sup>78</sup> Cations other than  $NH_4^+$  in a dilute alkali

solution prevent surface protonation by water, thereby decreasing the IN efficiency in feldspars.<sup>40</sup> On the other hand,  $\text{NH}_4^+$  causes improved ice nucleation possibly by chemical adsorption on the surface rather than ion exchange on the surface.<sup>22,40</sup> This enhancement is probably because of a better orientation of water molecules into ice-like layers by hydrogen-bonded  $\text{NH}_4^+$  or  $\text{NH}_3$  with the surface hydroxyl groups. This explanation is inferred because of the dependence of ammonium solute concentration on the ice nucleation, i.e., dilute solutions enhance IN efficiency, whereas high concentrations reduce IN efficiency.<sup>40,69,73</sup> High concentration of any solute results in adsorption of cations on the surface that may block nucleation sites which leads to decrease in IN efficiency in the order  $\text{NH}_4^+ > \text{Na}^+ > \text{K}^+$ .<sup>22</sup> Another experimental study to investigate the cation specific effect demonstrated that the IN efficiency decreased in the order of  $\text{H}^+ > \text{Cs}^+ > \text{Rb}^+ > \text{K}^+ > \text{Na}^+$  on mica surface.<sup>79</sup> Adsorption ability followed the sequence of  $\text{Ca}^{2+} > \text{Mg}^{2+} > \text{K}^+ > \text{Na}^+ > \text{Li}^+$  on montmorillonite and illite surfaces,<sup>80</sup> and  $\text{Cs}^+ > \text{K}^+ > \text{Na}^+$  on mica surfaces<sup>81</sup> shown by modeling studies that could also determine relative IN efficiency. Additional studies are needed to determine the exact reason for the decreased ice nucleation of the ammonium terminated zeolite surface as compared with the proton terminated zeolite surface as well as alkali ions.

### **Conclusion and Atmospheric implications:**

Four samples of ZSM-5 zeolite were used to determine the immersion freezing nucleation temperatures with decreasing Si:Al ratios. The results show remarkable increases in ice nucleation activity when there is a lower Si:Al ratio at the surface of the zeolite framework. This correlation between ice nucleation activity and Si:Al ratio is not observed with the bulk ratios reported by the manufacturers, demonstrating the need to understand the surface properties of a material to characterize the ice nucleation activity. Our work agrees with ice nucleation literature on

aluminosilicate minerals, which suggests that Al surfaces contribute more to ice nucleation activity than Si surfaces.

Additionally, the enhanced ice nucleation activity of ZSM-5 samples with low surface Si:Al ratios is diminished in the presence of ammonium as a cation compared with a proton cation. These findings suggest that tetrahedral aluminum interacts favorably with water at the particle interface to promote ice nucleation, and that aluminum active sites can be blocked or modified by the strong interaction with ammonium to reduce activity. Further work in this area is needed to fully understand exactly why the ammonium cation reduces the ice nucleation activity.

Since aluminosilicates are ubiquitous in the atmosphere, as are protons and ammonium, it is critical to further our understanding of the interaction of these components with water as they relate to ice nucleation. The effect of the features of heterogeneous surfaces on immersion freezing is important because it is a significant pathway for ice formation in the atmosphere, and influences cloud processes and radiative flux.

### **Conflicts of Interest**

There are no conflicts to declare.

### **Acknowledgements**

We thank E. A. Bazilevskaya and J. Shallenberger from the Materials Characterization Lab at the Pennsylvania State University for BET and XPS data and analysis. We gratefully acknowledge support from NSF grant CHE-1904803. K. E. M. additionally acknowledges support from NSF grant DGE-1255832.

### **References:**

- (1) Cziczo, D. J.; Froyd, K. D.; Hoose, C.; Jensen, E. J.; Diao, M.; Zondlo, M. A.; Smith, J. B.; Twohy, C. H.; Murphy, D. M. Clarifying the Dominant Sources and Mechanisms of Cirrus Cloud Formation. *Science* (80-. ). **2013**, *340* (6138), 1320–1324.
- (2) Zondlo, M. A.; Hudson, P. K.; Prenni, A. J.; Tolbert, M. A. Chemistry and Microphysics of Polar Stratospheric Clouds and Cirrus Clouds. *Annu. Rev. Phys. Chem.* **2000**, *51* (1), 473–499. <https://doi.org/10.1146/annurev.physchem.51.1.473>.
- (3) Yi, B.; Rapp, A. D.; Yang, P.; Baum, B. A.; King, M. D. A Comparison of Aqua MODIS Ice and Liquid Water Cloud Physical and Optical Properties between Collection 6 and Collection 5.1: Pixel-to-Pixel Comparisons. *J. Geophys. Res. Atmos.* **2017**, *122*, 4528–4549. <https://doi.org/10.1002/2016JD025586>.
- (4) Hoose, C.; Mohler, O. Heterogeneous Ice Nucleation on Atmospheric Aerosols: A Review of Results from Laboratory Experiments. *Atmos. Chem. Phys.* **2012**, *12*, 9817–9854. <https://doi.org/10.5194/acp-12-9817-2012>.
- (5) Ward, P. J.; DeMott, P. J. Preliminary Experimental Evaluation of Snomax (TM) Snow Inducer, Nucleus *Pseudomonas Syringae*, as an Artificial Ice for Weather Modification. *J. Weather Modif.* **1989**, *21* (1 SE-Scientific Papers), 9–13. <https://doi.org/10.54782/jwm.v21i1.351>.
- (6) Pruppacher, H. R.; Klett, P. J. D. *Diffusion Growth and Evaporation of Water Drops and Snow Crystals*; 2010. [https://doi.org/10.1007/0-306-48100-6\\_13](https://doi.org/10.1007/0-306-48100-6_13).
- (7) Chong, E.; King, M.; Marak, K. E.; Freedman, M. A. The Effect of Crystallinity and Crystal Structure on the Immersion Freezing of Alumina. *J. Phys. Chem. A* **2019**, *123* (12), 2447–2456. <https://doi.org/10.1021/acs.jpca.8b12258>.
- (8) Marak, K. E.; Roebuck, J. H.; Chong, E.; Poitras, H.; Freedman, M. A. Silica as a Model Ice-Nucleating Particle to Study the Effects of Crystallinity, Porosity, and Low-Density Surface Functional Groups on Immersion Freezing. *J. Phys. Chem. A* **2022**, *126*, 5965–5973. <https://doi.org/10.1021/acs.jpca.2c03063>.
- (9) Alstadt, V. J.; Dawson, J. N.; Losey, D. J.; Sihvonen, S. K.; Freedman, M. A. Heterogeneous Freezing of Carbon Nanotubes: A Model System for Pore Condensation and Freezing in the Atmosphere. *J. Phys. Chem. A* **2017**, *121* (42), 8166–8175. <https://doi.org/10.1021/acs.jpca.7b06359>.
- (10) Vali, G.; DeMott, P. J.; Möhler, O.; Whale, T. F. Technical Note: A Proposal for Ice Nucleation Terminology. *Atmos. Chem. Phys.* **2015**, *15* (18), 10263–10270. <https://doi.org/10.5194/acp-15-10263-2015>.
- (11) Kanji, Z. A.; Ladino, L. A.; Wex, H.; Boose, Y.; Burkert-Kohn, M.; Cziczo, D. J.; Krämer, M. Overview of Ice Nucleating Particles. *Meteorol. Monogr.* **2017**, *58* (1), 1.1-1.33. <https://doi.org/10.1175/amsmonographs-d-16-0006.1>.
- (12) Marcolli, C. Deposition Nucleation Viewed as Homogeneous or Immersion Freezing in Pores and Cavities. *Atmos. Chem. Phys.* **2014**, *14* (4), 2071–2104. <https://doi.org/10.5194/acp-14-2071-2014>.
- (13) Scheuvs, D.; Kandler, K. On Composition, Morphology, and Size Distribution of

- Airborne Mineral Dust BT - Mineral Dust: A Key Player in the Earth System; Knippertz, P., Stuut, J.-B. W., Eds.; Springer Netherlands: Dordrecht, 2014; pp 15–49. [https://doi.org/10.1007/978-94-017-8978-3\\_2](https://doi.org/10.1007/978-94-017-8978-3_2).
- (14) Peckhaus, A.; Kiselev, A.; Hiron, T.; Ebert, M.; Leisner, T. A Comparative Study of K-Rich and Na/Ca-Rich Feldspar Ice-Nucleating Particles in a Nanoliter Droplet Freezing Assay. *Atmos. Chem. Phys.* **2016**, *16* (18), 11477–11496. <https://doi.org/10.5194/acp-16-11477-2016>.
  - (15) Pach, E.; Verdaguer, A. Pores Dominate Ice Nucleation on Feldspars. *J. Phys. Chem. C* **2019**, *123* (34), 20998–21004. <https://doi.org/10.1021/acs.jpcc.9b05845>.
  - (16) Keinert, A.; Deck, K.; Gaedeke, T.; Leisner, T.; Kiselev, A. A. Mechanism of Ice Nucleation in Liquid Water on Alkali Feldspars. *Faraday Discuss.* **2022**, *235* (0), 148–161. <https://doi.org/10.1039/D1FD00115A>.
  - (17) Friddle, R. W.; Thürmer, K. How Nanoscale Surface Steps Promote Ice Growth on Feldspar: Microscopy Observation of Morphology-Enhanced Condensation and Freezing. *Nanoscale* **2019**, *11* (44), 21147–21154. <https://doi.org/10.1039/C9NR08729J>.
  - (18) Kiselev, A.; Bachmann, F.; Pedevilla, P.; Cox, S. J.; Michaelides, A.; Gerthsen, D.; Leisner, T. Active Sites in Heterogeneous Ice Nucleation—the Example of K-Rich Feldspars. *Science (80-. )*. **2017**, *355* (6323), 367–371. <https://doi.org/10.1126/science.aai8034>.
  - (19) Atkinson, J. D.; Murray, B. J.; Woodhouse, M. T.; Whale, T. F.; Baustian, K. J.; Carslaw, K. S.; Dobbie, S.; Sullivan, D. O.; Malkin, T. L. The Importance of Feldspar for Ice Nucleation by Mineral Dust in Mixed-Phase Clouds. *Nature* **2013**, *498*, 355–358. <https://doi.org/10.1038/nature12278>.
  - (20) Welti, A.; Lohmann, U.; Kanji, Z. A. Ice Nucleation Properties of K-Feldspar Polymorphs and Plagioclase Feldspars. *Atmos. Chem. Phys.* **2019**, *19* (16), 10901–10918. <https://doi.org/10.5194/acp-19-10901-2019>.
  - (21) Zolles, T.; Burkart, J.; Häusler, T.; Pummer, B.; Hitzenberger, R.; Grothe, H. Identification of Ice Nucleation Active Sites on Feldspar Dust Particles. *J. Phys. Chem. A* **2015**, *119* (11), 2692–2700. <https://doi.org/10.1021/jp509839x>.
  - (22) Kumar, A.; Marcolli, C.; Peter, T. Ice Nucleation Activity of Silicates and Aluminosilicates in Pure Water and Aqueous Solutions-Part 1: The K-Feldspar Microcline. *Atmos. Chem. Phys.* **2018**, *18* (10), 7057–7079. <https://doi.org/10.5194/acp-19-6059-2019>.
  - (23) Harrison, A. D.; Whale, T. F.; Carpenter, M. A.; Holden, M. A.; Neve, L.; Sullivan, D. O.; Temprado, J. V.; Murray, B. J. Not All Feldspars Are Equal: A Survey of Ice Nucleating Properties across the Feldspar Group of Minerals. *Atmos. Chem. Phys.* **2016**, *16*, 10927–10940. <https://doi.org/10.5194/acp-16-10927-2016>.
  - (24) Croteau, T.; Bertram, A. K.; Patey, G. N. Adsorption and Structure of Water on Kaolinite Surfaces: Possible Insight into Ice Nucleation from Grand Canonical Monte Carlo Calculations. *J. Phys. Chem. A* **2008**, *112* (43), 10708–10712. <https://doi.org/10.1021/jp805615q>.
  - (25) Ren, Y.; Bertram, A. K.; Patey, G. N. Effects of Inorganic Ions on Ice Nucleation by the Al

- Surface of Kaolinite Immersed in Water. *J. Phys. Chem. B* **2020**, *124* (22), 4605–4618. <https://doi.org/10.1021/acs.jpcc.0c01695>.
- (26) Sosso, G. C.; Li, T.; Donadio, D.; Tribello, G. A.; Michaelides, A. Microscopic Mechanism and Kinetics of Ice Formation at Complex Interfaces: Zooming in on Kaolinite. *J. Phys. Chem. Lett.* **2016**, *7* (13), 2350–2355. <https://doi.org/10.1021/acs.jpcclett.6b01013>.
- (27) Zielke, S. A.; Bertram, A. K.; Patey, G. N. Simulations of Ice Nucleation by Kaolinite (001) with Rigid and Flexible Surfaces. *J. Phys. Chem. B* **2016**, *120* (8), 1726–1734. <https://doi.org/10.1021/acs.jpcc.5b09052>.
- (28) Freedman, M. A. Potential Sites for Ice Nucleation on Aluminosilicate Clay Minerals and Related Materials. *J. Phys. Chem. Lett.* **2015**, *6* (19), 3850–3858. <https://doi.org/10.1021/acs.jpcclett.5b01326>.
- (29) Sihvonen, S. K.; Murphy, K. A.; Washton, N. M.; Altaf, M. B.; Mueller, K. T.; Freedman, M. A. Effect of Acid on Surface Hydroxyl Groups on Kaolinite and Montmorillonite. *Zeitschrift für Phys. Chemie* **2018**, *232* (3), 409–430. <https://doi.org/10.1515/zpch-2016-0958>.
- (30) Sihvonen, S. K.; Schill, G. P.; Lykтей, N. A.; Veghte, D. P.; Tolbert, M. A.; Freedman, M. A. Chemical and Physical Transformations of Aluminosilicate Clay Minerals Due to Acid Treatment and Consequences for Heterogeneous Ice Nucleation. *J. Phys. Chem. A* **2014**, *118*, 8787–8796. <https://doi.org/10.1021/jp504846g>.
- (31) Lüönd, F.; Stetzer, O.; Welti, A.; Lohmann, U. Experimental Study on the Ice Nucleation Ability of Size - Selected Kaolinite Particles in the Immersion Mode. *J. Geophys. Res. Atmos.* **2010**, *115* (D14), 1–14. <https://doi.org/10.1029/2009JD012959>.
- (32) Pinti, V.; Marcolli, C.; Zobrist, B.; Hoyle, C. R.; Peter, T. Ice Nucleation Efficiency of Clay Minerals in the Immersion Mode. *Atmos. Chem. Phys.* **2012**, *12*, 5859–5878. <https://doi.org/10.5194/acp-12-5859-2012>.
- (33) Welti, A.; Luond, F.; Kanji, Z. A.; Stetzer, O.; Lohmann, U. Time Dependence of Immersion Freezing : An Experimental Study on Size Selected Kaolinite Particles. *Atmos. Chem. Phys.* **2012**, *12*, 9893–9907. <https://doi.org/10.5194/acp-12-9893-2012>.
- (34) Hartmann, S.; Wex, H.; Clauss, T.; Augustin-Bauditz, S.; Niedermeier, D.; Rösch, M.; Stratmann, F. Immersion Freezing of Kaolinite: Scaling with Particle Surface Area. *J. Atmos. Sci.* **2016**, *73* (1), 263–278. <https://doi.org/10.1175/JAS-D-15-0057.1>.
- (35) Klumpp, K.; Marcolli, C.; Alonso-Hellweg, A.; Dreimol, C. H.; Peter, T. Comparing the Ice Nucleation Properties of the Kaolin Minerals Kaolinite and Halloysite. *Atmos. Chem. Phys.* **2023**, *23*, 1579–1598.
- (36) Grim, R. E. Clay Mineralogy. *Science* (80-. ). **1962**, *135* (3507), 890–898.
- (37) Soni, A.; Patey, G. N. How Microscopic Features of Mineral Surfaces Critically Influence Heterogeneous Ice Nucleation. *J. Phys. Chem. C* **2021**, *125* (19), 10723–10737. <https://doi.org/10.1021/acs.jpcc.1c01740>.
- (38) Hu, X. L.; Michaelides, A. Ice Formation on Kaolinite: Lattice Match or Amphotericism?



- Surf. Sci.* **2007**, *601* (23), 5378–5381. <https://doi.org/10.1016/j.susc.2007.09.012>.
- (39) Cox, S. J.; Raza, Z.; Kathmann, S. M.; Slater, B.; Michaelides, A. The Microscopic Features of Heterogeneous Ice Nucleation May Affect the Macroscopic Morphology of Atmospheric Ice Crystals. *Faraday Discuss.* **2013**, *167*, 389–403. <https://doi.org/10.1039/c3fd00059a>.
- (40) Kumar, A.; Marcolli, C.; Peter, T. Ice Nucleation Activity of Silicates and Aluminosilicates in Pure Water and Aqueous Solutions-Part 3: Aluminosilicates. *Atmos. Chem. Phys.* **2019**, *19* (9), 6059–6084. <https://doi.org/10.5194/acp-19-6059-2019>.
- (41) Hu, X. L.; Michaelides, A. Surface Science The Kaolinite (001) Polar Basal Plane. *Surf. Sci.* **2010**, *604* (2), 111–117. <https://doi.org/10.1016/j.susc.2009.10.026>.
- (42) Ren, Y.; Bertram, A. K. SI for The Influence of PH on Ice Nucleation by Kaolinite: Experiments and Molecular Simulations. *J. Phys. Chem. A* **2022**, 1–23.
- (43) Wang, B.; Knopf, D. A.; China, S.; Arey, B. W.; Harder, T. H.; Gilles, M. K.; Laskin, A. Direct Observation of Ice Nucleation Events on Individual Atmospheric Particles. *Phys. Chem. Chem. Phys.* **2016**, *18*, 29721–29731. <https://doi.org/10.1039/c6cp05253c>.
- (44) Wang, M.; Zhong, J.; Stacchiola, D. J.; Boscoboinik, J. A.; Lu, D. First-Principles Study of Interface Structures and Charge Rearrangement at the Aluminosilicate/Ru(0001) Heterojunction. *J. Phys. Chem. C* **2019**, *123*, 7731–7739 Article. <https://doi.org/10.1021/acs.jpcc.8b05853>.
- (45) Moura, P. A. S.; Rodríguez-aguado, E.; Maia, D. A. S.; Melo, D. C.; Singh, R.; Valencia, S.; Webley, A.; Rey, F.; Bastos-Neto, M.; Rodríguez-Castell'on, E.; Azevedo, D. C. S. Water Adsorption and Hydrothermal Stability of CHA Zeolites with Different Si / Al Ratios and Compensating Cations. *Catal. Today* **2022**, *391* (July 2021), 99–108. <https://doi.org/10.1016/j.cattod.2021.11.042>.
- (46) G. T. Kokotailo; S. L. Lawton; D. H. Olson; W. M. Meier. Structure of Synthetic Zeolite ZSM-5. *Nature* **1978**, *272* (March), 437–438.
- (47) *Zeolite Microporous Solids: Synthesis, Structure, and Reactivity*, 1st ed.; Derouane, E. G., Lemos, F., Naccache, C., Ribeiro, F. R., Eds.; Springer Dordrecht, 1992. <https://doi.org/https://doi.org/10.1007/978-94-011-2604-5>.
- (48) IZA Commission on Natural Zeolites <http://www.iza-online.org/natural/default.htm>.
- (49) Erdem, E.; Karapinar, N.; Donat, R. The Removal of Heavy Metal Cations by Natural Zeolites. *J. Colloid Interface Sci.* **2004**, *280* (2), 309–314. <https://doi.org/https://doi.org/10.1016/j.jcis.2004.08.028>.
- (50) Mumpton, F. A. La Roca Magica: Uses of Natural Zeolites in Agriculture and Industry. *Proc. Natl. Acad. Sci. U. S. A.* **1999**, *96* (7), 3463–3470. <https://doi.org/10.1073/pnas.96.7.3463>.
- (51) Ackley, M. W.; Rege, S. U.; Saxena, H. Application of Natural Zeolites in the Purification and Separation of Gases. *Microporous Mesoporous Mater.* **2003**, *61* (1), 25–42. [https://doi.org/https://doi.org/10.1016/S1387-1811\(03\)00353-6](https://doi.org/https://doi.org/10.1016/S1387-1811(03)00353-6).

- (52) Wang, S.; Peng, Y. Natural Zeolites as Effective Adsorbents in Water and Wastewater Treatment. *Chem. Eng. J.* **2010**, *156* (1), 11–24. <https://doi.org/https://doi.org/10.1016/j.cej.2009.10.029>.
- (53) Earl, D. J.; Deem, M. W. Toward a Database of Hypothetical Zeolite Structures. *Ind. Eng. Chem. Res.* **2006**, *45* (16), 5449–5454. <https://doi.org/10.1021/ie0510728>.
- (54) Baerlocher, C. H.; McCusker, L. B. <http://www.iza-structure.org/databases>.
- (55) Janssen, A. H.; Talsma, H.; Van Steenberghe, M. J.; De Jong, K. P. Homogeneous Nucleation of Water in Mesoporous Zeolite Cavities. *Langmuir* **2004**, *20* (1), 41–45. <https://doi.org/10.1021/la034340k>.
- (56) Derouane, E. G.; Gabelica, Z. A Novel Effect of Shape Selectivity: Molecular Traffic Control in Zeolite ZSM-5. *J. Catal.* **1980**, *65* (2), 486–489. [https://doi.org/https://doi.org/10.1016/0021-9517\(80\)90328-0](https://doi.org/https://doi.org/10.1016/0021-9517(80)90328-0).
- (57) von Ballmoos, R.; Meier, W. M. Zoned Aluminium Distribution in Synthetic Zeolite ZSM-5. *Nature* **1981**, *289* (5800), 782–783. <https://doi.org/10.1038/289782a0>.
- (58) Shirazi, L.; Jamshidi, E.; Ghasemi, M. R. The Effect of Si/Al Ratio of ZSM-5 Zeolite on Its Morphology, Acidity and Crystal Size. *Cryst. Res. Technol.* **2008**, *43* (12), 1300–1306. <https://doi.org/https://doi.org/10.1002/crat.200800149>.
- (59) O’Sullivan, D.; Murray, B. J.; Ross, J. F.; Whale, T. F.; Price, H. C.; Atkinson, J. D.; Umo, N. S.; Webb, M. E. The Relevance of Nanoscale Biological Fragments for Ice Nucleation in Clouds. *Sci. Rep.* **2015**, *5*, 1–7. <https://doi.org/10.1038/srep08082>.
- (60) Vali, G. Quantitative Evaluation of Experimental Results on the Heterogeneous Freezing Nucleation of Supercooled Liquids. *J. Atmos. Sci.* **1971**, *28*, 402–409.
- (61) Suzuki, Y.; Steinhart, M.; Butt, H.-J.; Floudas, G. Kinetics of Ice Nucleation Confined in Nanoporous Alumina. *J. Phys. Chem. B* **2015**, *119* (35), 11960–11966. <https://doi.org/10.1021/acs.jpcc.5b06295>.
- (62) Haag, W. O.; Lago, R. M.; Weisz, P. B. The Active Site of Acidic Aluminosilicate Catalysts. *Nature* **1984**, *309* (5969), 589–591. <https://doi.org/10.1038/309589a0>.
- (63) Murray, B. J.; Broadley, S. L.; Wilson, T. W.; Atkinson, J. D.; Wills, R. H. Heterogeneous Freezing of Water Droplets Containing Kaolinite Particles. *Atmos. Chem. Phys.* **2011**, *11*, 4191–4207. <https://doi.org/10.5194/acp-11-4191-2011>.
- (64) Harrison, A. D.; Lever, K.; Sanchez-Marroquin, A.; Holden, M. A.; Whale, T. F.; Tarn, M. D.; McQuaid, J. B.; Murray, B. J. The Ice-Nucleating Ability of Quartz Immersed in Water and Its Atmospheric Importance Compared to K-Feldspar. *Atmos. Chem. Phys.* **2019**, *19*, 11343–11361.
- (65) Holden, M. A.; Whale, T. F.; Tarn, M. D.; Sullivan, D. O.; Walshaw, R. D.; Murray, B. J.; Meldrum, F. C.; Christenson, H. K. High-Speed Imaging of Ice Nucleation in Water Proves the Existence of Active Sites. *Sci. Adv.* **2019**, *5*, 1–10.
- (66) Kumar, A.; Marcolli, C.; Peter, T. Ice Nucleation Activity of Silicates and Aluminosilicates

- in Pure Water and Aqueous Solutions-Part 2: Quartz and Amorphous Silica. *Atmos. Chem. Phys.* **2019**, *19* (9), 6035–6058. <https://doi.org/10.5194/acp-19-6035-2019>.
- (67) Losey, D. J.; Sihvonen, S. K.; Veghte, D. P.; Chong, E.; Freedman, M. A. Acidic Processing of Fly Ash: Chemical Characterization, Morphology, and Immersion Freezing. *Environ. Sci. Process. Impacts* **2018**, *20* (11), 1581–1592. <https://doi.org/10.1039/c8em00319j>.
- (68) Hiranuma, N.; Augustin-Bauditz, S.; Bingemer, H.; Budke, C.; Curtius, J.; Danielczok, A.; Diehl, K.; Dreischmeier, K.; Ebert, M.; Frank, F.; Hoffmann, N.; Kandler, K.; Kiselev, A.; Koop, T.; Leisner, T.; Möhler, O.; Nillius, B.; Peckhaus, A.; Rose, D.; Weinbruch, S.; Wex, H.; Boose, Y.; Demott, P. J.; Hader, J. D.; Hill, T. C. J.; Kanji, Z. A.; Kulkarni, G.; Levin, E. J. T.; McCluskey, C. S.; Murakami, M.; Murray, B. J.; Niedermeier, D.; Petters, M. D.; O'Sullivan, D.; Saito, A.; Schill, G. P.; Tajiri, T.; Tolbert, M. A.; Welti, A.; Whale, T. F.; Wright, T. P.; Yamashita, K. A Comprehensive Laboratory Study on the Immersion Freezing Behavior of Illite NX Particles: A Comparison of 17 Ice Nucleation Measurement Techniques. *Atmos. Chem. Phys.* **2015**, *15* (5), 2489–2518. <https://doi.org/10.5194/acp-15-2489-2015>.
- (69) Whale, T. F.; Holden, M. A.; Wilson, T. W.; O'Sullivan, D.; Murray, B. J. The Enhancement and Suppression of Immersion Mode Heterogeneous Ice-Nucleation by Solutes. *Chem. Sci.* **2018**, *9* (17), 4142–4151. <https://doi.org/10.1039/c7sc05421a>.
- (70) Whale, T. F. Disordering Effect of the Ammonium Cation Accounts for Anomalous Enhancement of Heterogeneous Ice Nucleation. *J. Chem. Phys.* **2022**, *156* (14), 144503. <https://doi.org/10.1063/5.0084635>.
- (71) Cox, S. J.; Kathmann, S. M.; Slater, B.; Michaelides, A. Molecular Simulations of Heterogeneous Ice Nucleation I: Controlling Ice Nucleation through Surface Hydrophilicity. *J. Chem. Phys.* **2015**, *142*, 184704.
- (72) Takeuchi, M.; Tsukamoto, T.; Kondo, A.; Matsuoka, M. Investigation of NH<sub>3</sub> and NH<sub>4</sub><sup>+</sup> Adsorbed on ZSM-5 Zeolites by near and Middle Infrared Spectroscopy. *Catal. Sci. Technol.* **2015**, *5* (9), 4587–4593. <https://doi.org/10.1039/C5CY00753D>.
- (73) Worthy, S. E.; Kumar, A.; Xi, Y.; Yun, J.; Chen, J.; Xu, C.; Irish, V. E.; Amato, P.; Bertram, A. K. The Effect of (NH<sub>4</sub>)<sub>2</sub>SO<sub>4</sub> on the Freezing Properties of Non-Mineral Dust Ice Nucleating Substances of Atmospheric Relevance. *Atmos. Chem. Phys. Discuss.* **2021**, No. March, 1–30.
- (74) Chen, J.; Wu, Z.; Meng, X.; Zhang, C.; Chen, J.; Qiu, Y.; Chen, L.; Fang, X.; Wang, Y.; Zhang, Y.; Chen, S.; Gao, J.; Li, W.; Hu, M. Observational Evidence for the Non-Suppression Effect of Atmospheric Chemical Modi Fi Cation on the Ice Nucleation Activity of East Asian Dust. *Sci. Total Environ.* **2023**, *861*, 160708. <https://doi.org/10.1016/j.scitotenv.2022.160708>.
- (75) Kumar, A.; Bertram, A. K.; Patey, G. N. Molecular Simulations of Feldspar Surfaces Interacting with Aqueous Inorganic Solutions: Interfacial Water/Ion Structure and Implications for Ice Nucleation. *ACS Earth Sp. Chem.* **2021**, *5* (8), 2169–2183. <https://doi.org/10.1021/acsearthspacechem.1c00216>.
- (76) Nihonyanagi, S.; Yamaguchi, S.; Tahara, T. Counterion Effect on Interfacial Water at

- Charged Interfaces and Its Relevance to the Hofmeister Series. *J. Am. Chem. Soc.* **2014**, *136* (17), 6155–6158.
- (77) Chen, X.; Yang, T.; Kataoka, S.; Cremer, P. S. Specific Ion Effects on Interfacial Water Structure near Macromolecules Second , How Do These Interactions Contribute to the Overall An Attractive Technique for Investigating Interfacial Water And. *J. Am. Chem. Soc.* **2007**, *129* (40), 12272–12279.
- (78) He, Z.; Xie, W. J.; Liu, Z.; Liu, G.; Wang, Z.; Gao, Y. Q.; Wang, J. Tuning Ice Nucleation with Counterions on Polyelectrolyte Brush Surfaces. *Sci. Adv.* **2016**, *2* (6), e1600345.
- (79) Jin, S.; Liu, Y.; Deiseroth, M.; Liu, J.; Backus, E. H. G.; Li, H.; Xue, H.; Zhao, L.; Zeng, X. C.; Bonn, M.; Wang, J. Use of Ion Exchange to Regulate the Heterogeneous Ice Nucleation Efficiency of Mica. *J. Am. Chem. Soc.* **2020**, *142* (42), 17956–17965. <https://doi.org/10.1021/jacs.0c00920>.
- (80) Liu, X.; Li, H.; Du, W.; Tian, R.; Li, R.; Jiang, X. Hofmeister Effects on Cation Exchange Equilibrium: Quantification of Ion Exchange Selectivity. *J. Phys. Chem. C* **2013**, *117* (12), 6245–6251.
- (81) Jia, Z.; Li, X.; Zhu, C.; Yang, S.; Yang, G. Reversal of Cation-Specific Effects at the Interface of Mica and Aqueous Solutions. *J. Phys. Chem. C* **2018**, *122* (10), 5358–5365. <https://doi.org/10.1021/acs.jpcc.7b09956>.